Journal of Power Sources 185 (2008) 1484–1491

Contents lists available at ScienceDirect

Journal of Power Sources

journal homepage: www.elsevier.com/locate/jpowsour

Lead acid batteries simulation including experimental validation

N. Achaibou[a,*], M. Haddadi[b], A. Malek[a]

[a] Division Energie Solaire Photovoltaïque, Centre de Développement des Energies Renouvelables, B.P. 62, Route de l'Observatoire, Bouzaréah, Alger, Algeria
[b] Laboratoire de Dispositif de Communication et de Conversion Photovoltaïque Ecole Nationale Polytechnique, Rue Hassen Badi, El Harrach, Alger, Algeria

ARTICLE INFO

Article history:
Received 16 April 2008
Received in revised form 7 June 2008
Accepted 22 June 2008
Available online 3 July 2008

Keywords:
Battery storage
Battery modelling
Lead acid battery
Storage system
PV system

ABSTRACT

The storage of energy in batteries is a cause of the failure and loss of reliability in PV systems. The battery behavior has been largely described in the literature by many authors; the selected models are of Monegon and CIEMAT. This paper reviews the two general lead acid battery models and their agreement with experimental data. In order to validate these models, the behavior of different battery cycling currents has been simulated. Results obtained have been compared to real data. The CIEMAT model presents a good performance compared to Monegon's model.

1. Introduction

Battery is a crucial component in a stand-alone photovoltaic system. It acts as a dumper by allowing the storage of excess energy from the PV array and, provides energy for the loads during night or non-sunny days. It can be considered as a stabilizer since it feeds the loads with constant voltage.

Batteries are used in most stand-alone PV systems, and are in many cases the least understood and the most vulnerable component of the system. They remain a complicated element, since they are the only dynamic element in a PV system. In fact many phenomena can occur such as charge and discharge. Many parameters vary during these processes such as voltage, current, density, temperature, resistivity, etc. This leads to a complicated behavior of this element and thus makes predictions of the state of charge much more complicated. Battery state of charge evaluation usually consists of measuring manually the electrolyte density; this method can only be employed by people in charge of the maintenance of an installation and is not feasible for a private individual wishing to have at least daily information.

The battery behavior has been largely described in the literature by many authors.

An important contribution was given by Shepherd [1]. The knowledge of internal battery processes permitted to derive an empirical equation which represents a wide variety of batteries in discharge and a complete set of discharge curves. This equation uses a minimum of experimental data for the parameters fitting. Besides, it includes an exponential term that gives an approximation of the potential drop at the beginning of discharge and another term associated with changes in the electrolyte concentration. Nevertheless, the applicability of this equation appears to be limited to average temperatures and it can be applied for battery charging if different values for parameters are used. Modifications to the Shepherd model were proposed by Hyman [2] to include low current effects for PV application, and were used by Facinelli [3] for a program to simulate solar systems. Other contributions appear in this work: temperature effects, a function for charging efficiency and a simple model for the battery lifetime. Other models were developed concerning the internal electrochemical, chemical and physical battery process. Mayer and Biscaglia [4], in a discharge model, used for the state of charge meter purpose, takes into account the over voltages corresponding to different phenomena. The equations for voltage, capacity and internal resistance depend on many parameters.

Most of the models require the knowledge of appropriate parameters, excepting the Monegon model [5] and CIEMAT model [6–9] do not keep the parameters fixed. Thereby, they must fit for each battery design, the values used in charge also differs from those used in discharge. They are non linear equations, which takes into account not only the charge and discharge but also the overcharge. It also necessitates few input parameters.

This paper reviews the calculations from the two general lead acid battery models and the agreement with a set of experimental data obtained from tests with a charge–discharge equipment. In order to validate these two models, the behavior of different

* Corresponding author. Tel.: +213 21 90 15 03; fax: +213 21 90 16 54.
E-mail address: n_achaibou@hotmail.com (N. Achaibou).

0378-7753/$ – see front matter © 2008 Elsevier B.V. All rights reserved.
doi:10.1016/j.jpowsour.2008.06.059

battery cycling currents has been simulated. Results obtained have been compared to real data gathered with charge–discharge equipment at currents typical in photovoltaic applications at ambient temperature (25 °C) for five different batteries.

2. Battery modeling

Sizing is one of the most important tasks during the design of a stand-alone PV system. The sizing procedure will determine the power rating of the PV array and the battery storage capacity needed to power the required load; the electrical configuration of the array may also be considered at this stage. More sophisticated sizing procedures will ensure that the reliability of power delivered to the load is appropriate for a given application and optimise the cost of the system. The availability of a mathematical model fitted to experimental data is important to understand better the behaviour of batteries along the life cycles in realistic conditions.

The battery is a complex electrochemical system. Some of its effects are imperfectly understood theoretically and although practical electrochemists know what works and what does not, there is still an element of art in the main electrochemical disciplines, including battery technology.

Only lead acid and to a small extent nickel-cadmium batteries are used in PV systems. Nickel-iron batteries are rarely used in any application, and suffer from a particularly high self-discharge rate that makes them unsuitable for most PV applications. Nickel-hydride and rechargeable lithium batteries are relatively modern developments whose main applications today are in high value electronic goods such as mobile phones and laptop computers. They are considerably more expensive today per kWh than lead acid batteries, and often need some rather sophisticated protection in their charging circuitry which is not easy to adapt to the changing nature of PV charge currents. There are other rechargeable battery types under development for such future battery applications as electric vehicles or load levelling. These are not commercially available yet, except in some limited cases.

A practical battery basically consists of the following items:

- A container.
- Positive and negative electrodes. Often called plates, these hold the different active material on some form of conducting support.
- An electrolyte (normally a liquid).
- Separators to stop the electrodes touching.
- Positive and negative connections to the external circuit.

The energy stored in a lead acid battery is chemical energy that can be converted into electrical energy during discharge and vice versa during re-charge. The positive electrode consists of lead oxide, the negative, lead. Both are converted to lead sulfate in the discharge process. The electrodes are immersed in sulfuric acid.

The chemical reactions follow the redox pattern. The current in the external circuit flows conventionally from the positive to the negative electrode. The two reactions can be written as follows [10,11]:

Positive:

$$PbO_2 + 4H^+ + {SO_4}^{2-} + 2e^- \rightarrow PbSO_4 + 2H_2O \quad (1)$$

Negative:

$$Pb + {SO_4}^{2-} \rightarrow PbSO_4 + 2e^- \quad (2)$$

The reversible potentials are $V_+ = +1.685$ V and $V_- = -0.356$ V, giving an open circuit e.m.f. $V = 2.041$ V.

During charging the reactions are:

Positive electrode:

$$PbSO_4 + 2(OH)^- \rightarrow PbO_2 + H_2SO_4 + 2e^- \quad (3)$$

Negative electrode:

$$PbSO_4 + 2H^+ + 2e^- \rightarrow Pb + H_2SO_4 \quad (4)$$

The fully charged cell has

positive	electrolyte	negative
PbO_2 (lead dioxide)	dilute H_2SO_4	Pb (spongy lead)

The overall cell reactions are

$$PbO_2 + 2H_2SO_4 + Pb \underset{\text{charge}}{\overset{\text{discharge}}{\rightleftarrows}} 2PbSO_4 + 2H_2O \quad (5)$$

This equation lies at the base of the so-called "theory of double sulphation" laid in 1884 by Gladstone and Trible [12].

During discharge the active parts of both electrodes are converted to lead sulphate, and the concentration of the electrolyte is reduced by both the removal of sulphate ions and the formation of water. During charge, the lead sulphate at the negative plate is reduced to spongy lead, and it is oxidised at the positive electrode to lead dioxide. There is a release of sulphate ions at both plates and therefore an increase in the concentration of the electrolyte. Measurement of the concentration indicates the state of the electrodes: the relative density of the electrolyte is read by a hydrometer.

Lead sulphate, the product of the discharge reaction, is practically insoluble in the electrolyte, a factor that endows the cell with its high degree of reversibility.

During cycling the lead sulphate remains where it is formed and the structure of the active materials is relatively undisturbed.

The modelling of electrochemical cells, secondary batteries or electrochemical energy storage devices in general has been widely published works available [1–14]. These works are sometimes based on empirical relationships, and other times on a detailed description of physical and chemical processes that take palace in cell, and even on the development of equivalent circuits. There is also a wide variety depending on the goals. There are isothermal models, thermal models include effect of temperature, and even age on cell performance, models that study the recombination of gases during the charge process.

Many models have been developed to describe the voltage evolution taking into account the variation of the internal resistance. Most of the proposed models based on the experimental identification of the intrinsic parameters for each type of battery. The advantage of the battery models developed by CIEMAT and Monegon is there ability to cope with a wider range of lead acid batteries and requires few manufacturers' data technological parameters.

The voltage of the battery reflects the different 'chemical potentials' of the two active materials when they react with the electrolyte—simplistically speaking, the more reactive the two materials, the higher will be the voltage of a battery they comprise. During the oxidation and reduction reactions, the active materials change into different chemical forms.

The simplest equation to represent the relationship between the voltage (V) the current (I) during charge and discharge is given by

$$V = V_{oc} \pm IR \quad (6)$$

where V_{oc} is the open circuit voltage and R is the internal resistance. The current I is positive during charge and negative during the discharge. The internal resistance is variable, and depends on other parameters such as capacity, charge/discharge current, temperature. The two models analyzed below describe the battery behaviour under the variation of the external characteristics: voltage, current, state of charge and temperature. Three processes are

Table 1
Batteries electrical proprieties

Battery type	Symbol	Nominal capacity (Ah)	Nominal voltage (V)
Varta solar	'Bat1'	100	12
ENPEC	'Bat2'	160	6
ENPEC	'Bat3'	80	12
Fulmen TXE 225	'Bat4'	220	2
Tudor STTH 180	'Bat5'	180	2

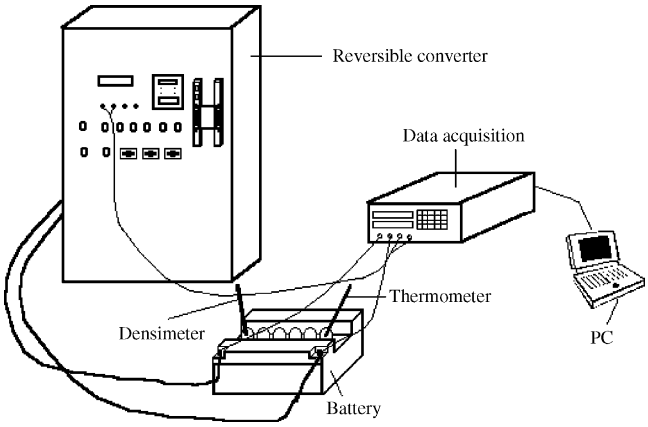

Fig. 1. Diagram of the experimental device.

considered: discharge, charge and overcharge, and their mathematical formulations are given as below.

2.1. CIEMAT model

This battery model is proposed as a tool to simulate and optimize PV storage systems. The normalized form of the equations with respect to the battery capacity allows us to generalize its use for any type and size of lead acid batteries [8].

2.1.1. Discharge voltage equation

The discharging is given by the following equation:

$$V = [2.085 - 0.12(1 - \mathrm{SOC})] - \frac{I}{C_{10}}\left(\frac{4}{1 + I^{1.3}} + \frac{0.27}{\mathrm{SOC}^{1.5}} + 0.02\right) \times (1 - 0.007\ \Delta T) \quad (7)$$

The first term represents the open circuit voltage variation with the state of charge (electrolyte concentration) and the second is due to the internal resistance variation which is represented by the sum of series resistances caused by other different phenomena.

Fig. 2. Photo of the experimental device.

Table 3
Charge and discharge current rate of the various types of battery

Bat1	Bat2	Bat3	Bat4	Bat5
Charge				
$I(C_5) = 20$	$I(C_{20}) = 8$	$I(C_{10}) = 8$	$I(C_5) = 44$	$I(C_{7.5}) = 24$
$I(C_{10}) = 10$	$I(C_{40}) = 4$	$I(C_{20}) = 4$	$I(C_{10}) = 22$	$I(C_{10}) = 18$
$I(C_{20}) = 5$			$I(C_{55}) = 4$	$I(C_{18}) = 10$
$I(C_{70}) = 1.4$				$I(C_{36}) = 5$
Discharge				
$I(C_5) = 20$	$I(C_{10}) = 16$	$I(C_{10}) = 8$	$I(C_5) = 44$	$I(C_{7.5}) = 24$
$I(C_{10}) = 10$	$I(C_{20}) = 8$	$I(C_{20}) = 4$	$I(C_{10}) = 22$	$I(C_{10}) = 18$
$I(C_{20}) = 5$	$I(C_{40}) = 4$	$I(C_{40}) = 2$	$I(C_{55}) = 4$	$I(C_{18}) = 10$
$I(C_{50}) = 2$	$I(C_{80}) = 2$			$I(C_{36}) = 5$
$I(C_{70}) = 1.4$				

Where the temperature variation is

$$\Delta T = T - 25 \quad (8)$$

Depth of discharge (DOD) is the fraction or percentage of the capacity which has been removed from the fully charged battery. Conversely, the state of charge (SOC) is the fraction or percentage of the capacity is still available in the battery. It is similar to considering whether a bucket (or drinking glass) is half empty or half full:

$$\mathrm{SOC} = 1 - \frac{Q}{C} \quad (9)$$

$$\mathrm{DOD} = \frac{Q}{C} \quad (10)$$

$$Q = It \quad (11)$$

Table 2
Batteries technical description

	'Bat1'	'Bat2'–'Bat3'	'Bat4'–'Bat5'
Positive plate	Flat with pocket	Tubular, matter	Tubular open type
Negative plate	Flat, alloy of grid; lead-antimony	Flat, alloy of grid; Lead-antimony	Flat, alloy with low antimony content
Container and lid	Container and the lid are heat-welded and electrolyte tight from shock-proof and stable plastic at the temperature	Container made of ebonite, the lid is adapted to seal tightly	Transparent container on visible level; explosion-proof stoppers and sintered ceramics discs
Separators	Microporous with low electrical resistance	Fine sheets of synthetic matter or cellulose, insulating and porous	Microporous with low electrical resistance
Maintenance	Minimal water consumption, which gives a long lifespan and a very small maintenance	The reserve of electrolyte is not significant enough	Large reserve of electrolyte (very low maintenance, long lifespan)
Dimensions (mm): $L^* \times L^* \times H$	$372^* \times 175^* \times 195$	$400^* \times 150^* \times 190$	$210^* \times 100^* \times 400$ $198^* \times 189^* \times 380$
Weight (kg) dry	18	18–32	17–16

The efficiency during discharge is assumed to be 100%; however, the total amount of useful charge available during discharge is limited by the current rate and temperature given by the capacity. This last is normalized with respect to discharge current corresponding to C_{10} rated capacity (I_{10}) is

$$\frac{C}{C_{10}} = \frac{1.67}{1 + 0.67(I/I_{10})^{0.9}}(1 + 0.005\,\Delta T) \tag{12}$$

When the discharge current tends to zero, the maximum capacity that can be removed is about 67% over C_{10} capacity at 25 °C.

2.1.2. Charge voltage equation

The charging equation is given by the following equation:

$$V = [2 - 0.16\,\mathrm{SOC}] + \frac{I}{C_{10}}\left(\frac{6}{1 + I^{0.86}} + \frac{0.48}{(1 - \mathrm{SOC})^{1.2}} + 0.036\right) \times (1 - 0.025\ \Delta T) \tag{13}$$

In this case, the state of charge (SOC) is function of the efficiency conversion η_c and SOC_0:

$$\mathrm{SOC} = \mathrm{SOC}_0 + \frac{\eta_c Q}{C} \tag{14}$$

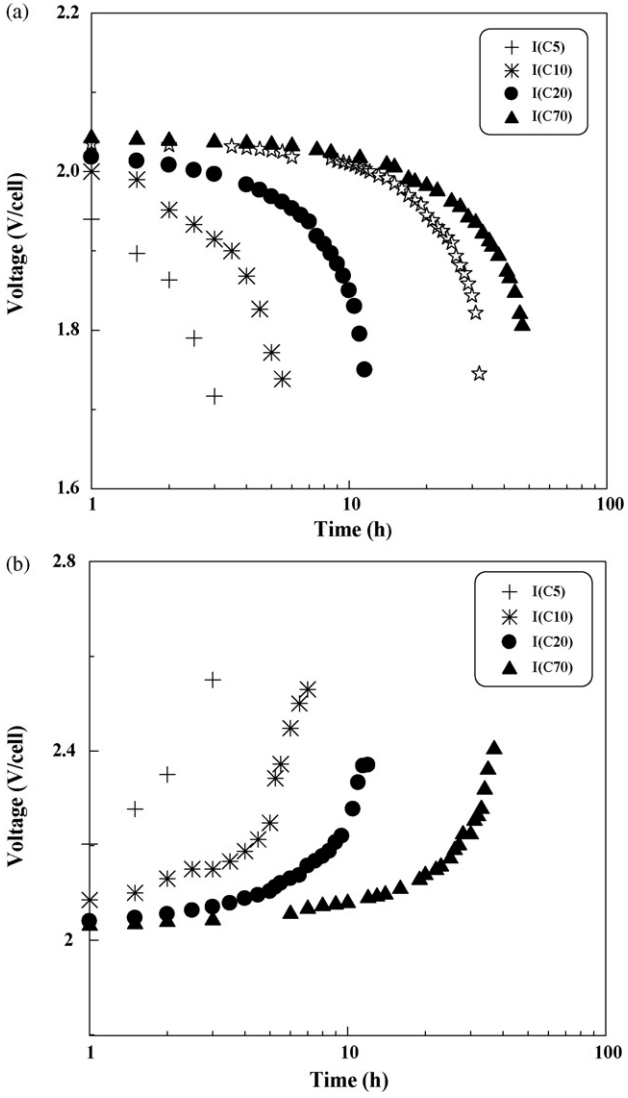

Fig. 3. Voltage versus time in charge and discharge at various currents and 25 °C for 'Bat1'. (a) Discharge; (b) Charge.

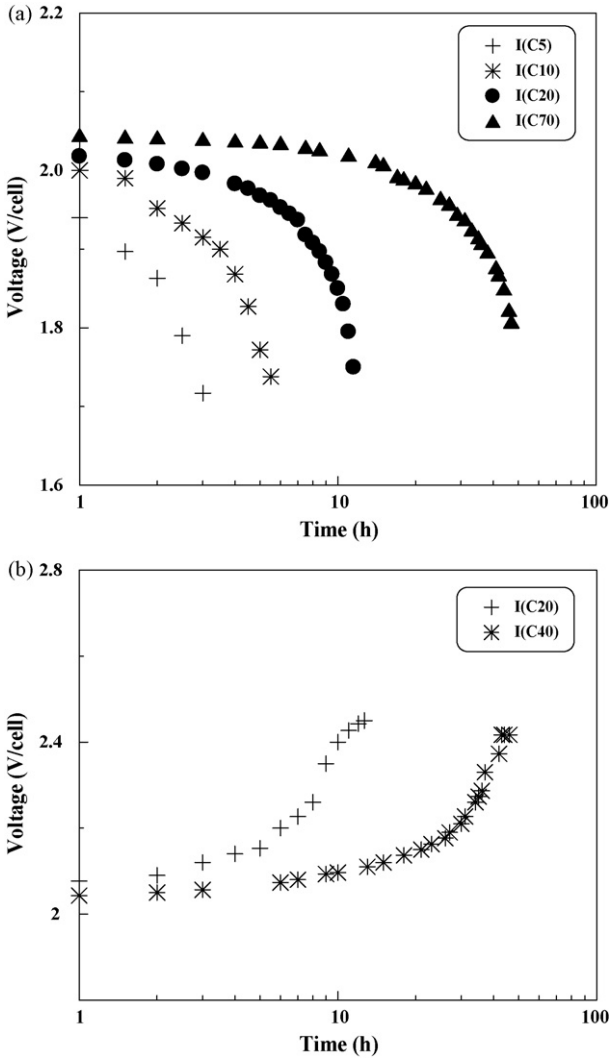

Fig. 4. Voltage versus time in charge and discharge at various currents and 25 °C for 'Bat2'. (a) Discharge; (b) Charge.

$$\eta_c = 1 - \exp\left[\frac{20.73}{I/I_{10} + 0.55}(\mathrm{SOC} - 1)\right] \tag{15}$$

2.1.3. Overcharge voltage equation

The overcharge can be represented by the following exponential function:

$$V = V_g + (V_{ec} - V_g)\left[1 - \exp\left(\frac{0.95C - \mathrm{Ah}_{\mathrm{restored}}}{I\tau}\right)\right] \tag{16}$$

where V_g and V_{ec} represent the gassing and final charge voltage, respectively

$$V_g = \left[2.24 + 1.97\ln\left(1 + \frac{I}{C_{10}}\right)\right](1 - 0.002\,\Delta T) \tag{17}$$

$$V_{ec} = \left[2.45 + 2.011\ln\left(1 + \frac{I}{C_{10}}\right)\right](1 - 0.002\,\Delta T) \tag{18}$$

$\mathrm{Ah}_{\mathrm{restored}}$ represents the ampere-hours stored in the battery with regard to the battery capacity C for the charge current I during this hour. It is assumed that 95% of the capacity is already restored at the start of the charge.

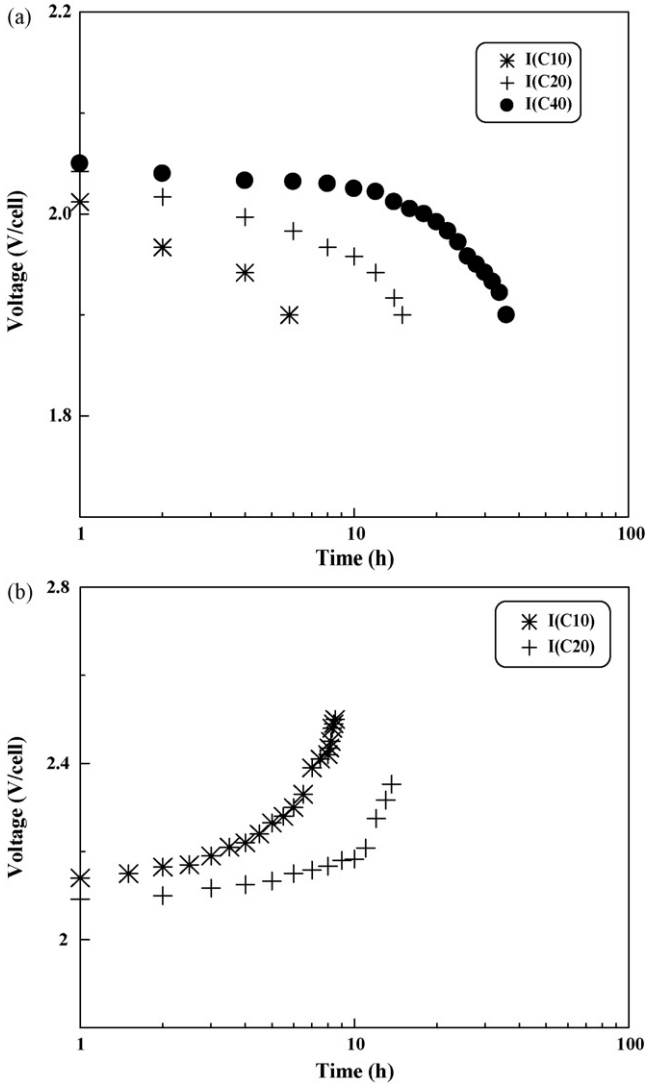

Fig. 5. Voltage versus time in charge and discharge at various currents and 25 °C for 'Bat3'. (a) Discharge; (b) Charge.

The time constant τ is inversely proportional to charge current intensity and, as an approximation, can be written as

$$\tau = \frac{17.3}{1 + 852(I/C_{10})^{1.67}} \tag{19}$$

2.2. Monegon model

In a report for photovoltaic stand-alone systems, presented by Monegon [2], the equations for battery charge and discharge are given in a normalized form with respect to the battery capacity, thus their parameters are fixed. Furthermore, the open circuit voltage and internal resistance are functions of the temperature and an attempt to represent the operate during overcharge is made.

2.2.1. Discharge voltage equation

$$V = 2.094(1 - 0.001(T - 25)) - \frac{I}{C_{10}}\left(\frac{0.189}{\text{SOC}} - 0.15(1 - 0.02(T - 25))\right) \tag{20}$$

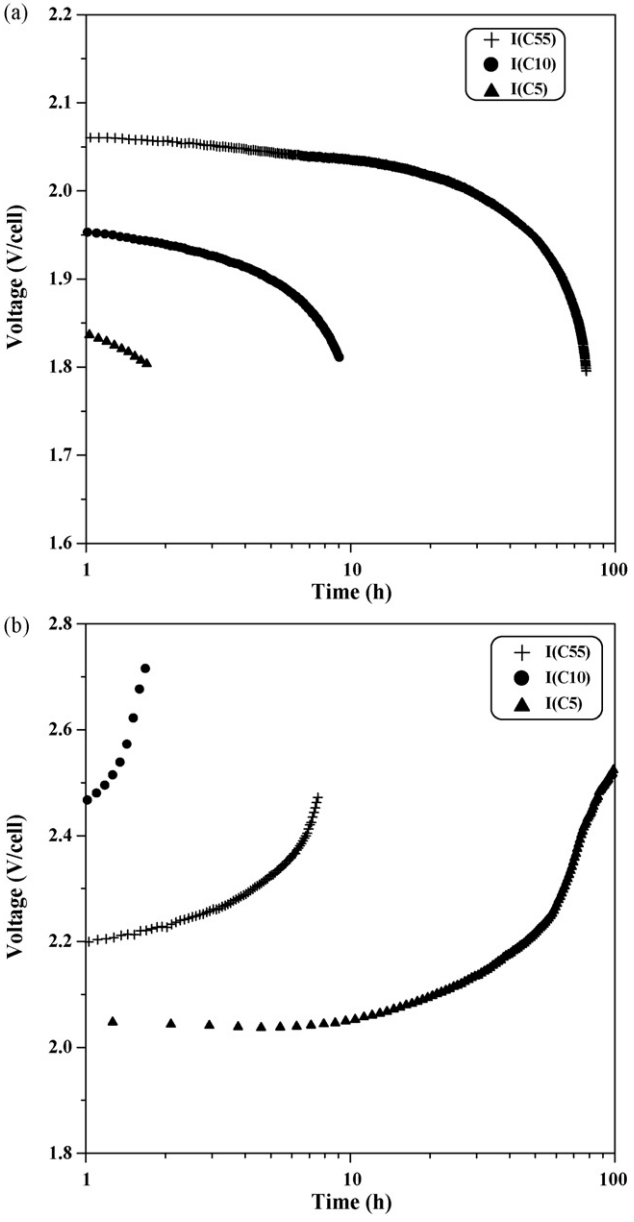

Fig. 6. Voltage versus time in charge and discharge at various currents and 25 °C for 'Bat4'. (a) Discharge; (b) Charge.

2.2.2. Charge voltage equation

$$V = 2.094(1 - 0.001(T - 25)) + \frac{I}{C_{10}}\left(\frac{0.189}{1.142 - \text{SOC}} + 0.15(1 - 0.02(T - 25))\right) \tag{21}$$

2.2.3. Overcharge voltage equation

$$V = 2.094(1 - 0.001(T - 25)) + \frac{I}{C_{10}}\left(\frac{0.189}{1.142 - \text{SOC}} + 0.15(1 - 0.02(T - 25))\right) + (\text{SOC} - 0.9)\ \ln\left(\frac{300I}{C_{10}} + 1\right) \tag{22}$$

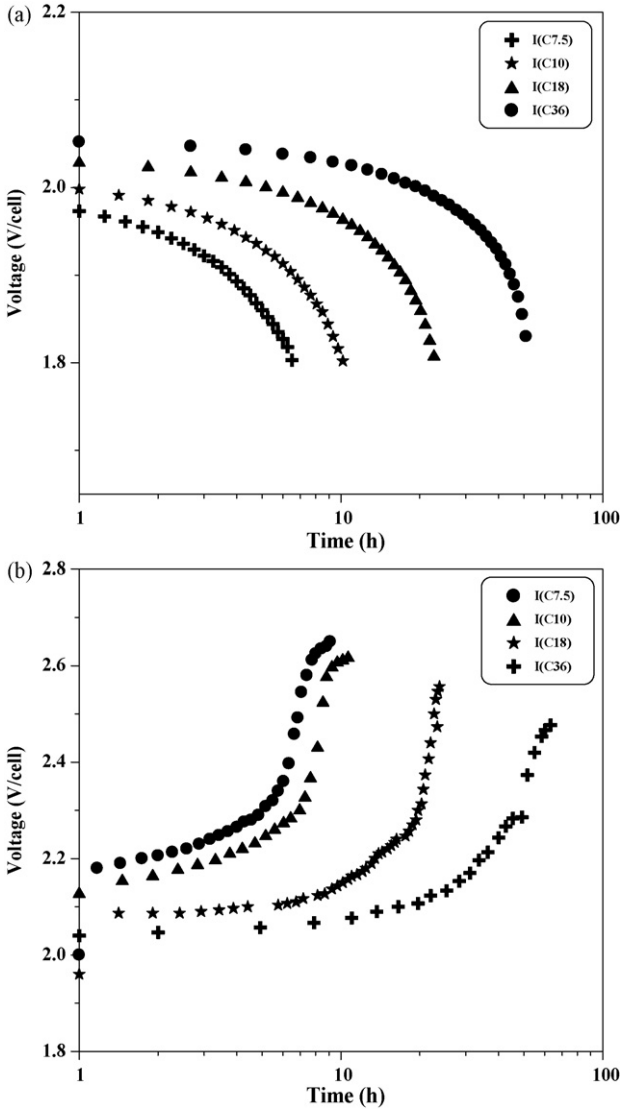

Fig. 7. Voltage versus time in charge and discharge at various currents and 25 °C for 'Bat5. (a) Discharge; (b) Charge.

3. Experiments and results

Battery discharge and charge tests were carried out upon lead acid batteries at different currents. All tests are carried out room temperature.

Within the framework of this experimental characterization, five types of lead acid batteries of various technologies and various manufacturers were chosen and tested [15]. Technical descriptions are given in Tables 1 and 2.

The tests which were carried out for the measurement of the characteristic parameters of the battery are as follows: charge process, discharge process, determination of the electrolyte density. The synoptic diagram of the experimental device is given in Figs. 1 and 2.

The tests of charge and discharge processes were carried out for various currents. The currents chosen in this study are suitable to cover the range operating conditions, including PV systems applications, see Table 3.

The results obtained of the densities, the tensions and the capacity are corrected at the temperature of 25 ° C using the following formulas [16]:

$$d_{25} = d + 0.0007(T - 25) \quad (23)$$

$$V_{25} = V + 0.005(T - 25) \quad (24)$$

$$C_{25} = \frac{C}{1 + 0.003(T - 25)} \quad (25)$$

The voltage and current were recorded periodically. Some of the results obtained for voltage versus time in charge and discharge at various currents and 25 °C for differents type of batteries are presented in Figs. 3–7:

Variation of the open circuit voltage according to the density of the electrolyte is given in Fig. 8.

The linear approximation of the experimental points gave for the type of battery 'Bat1' the following expression:

$$V_{oc} = 1.264d + 0.546 \quad (26)$$

Considering the batteries are new and consequently they do not present a sign of degradation, nor stratification, it is noted of these results that all energy is accumulated in the battery.

From the discharge curves, we calculate the capacities of the batteries for end of discharge voltage of 1.75 V/element for 'Bat1', 1.9 V/element for 'Bat2' and 'Bat3' and 1.8 V/element for 'Bat4' and 'Bat5', and from the charges curves we determine the values of V_g, t_g, V_{fc}, t_{fc}. Results are resumed in Table 4.

4. Models validation

For the implementation of the battery model described previously, the model is considered as a black box which is illustrated by the synopsis of the figure (Fig. 9).

The principle implementation consists in finding a solution of the battery model in order to determine the charge or discharge voltages. The battery was cycled from 30% to 100% for charge and from 100% to 30% for discharge at standard test condition $T = 25$ °C. Data is collected automatically via a data logger for both charge and discharge with different currents.

The comparison between real data and model simulation is presented in Figs. 10 and 11 for charge and discharge processes of 'Bat1'.

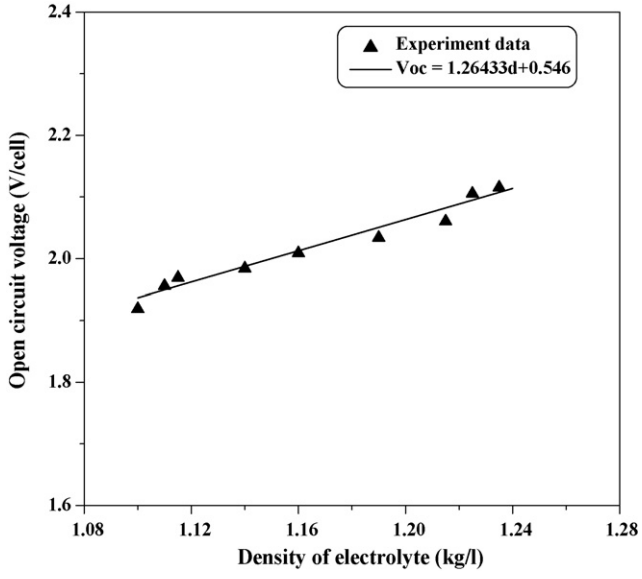

Fig. 8. Open circuit voltage according to the density of the electrolyte for 'Bat1'.

Table 4
Capacities, gassing voltage and final charge voltage according to the current for $T = 25\,^{\circ}C$

I (A)	C (Ah)	t_g	V_g	t_f	V_{fc}
'Bat1'					
20	60	2.222	2.341	4	2.606
10	64	5.179	2.187	10	2.567
5	65	9.540	2.135	18.42	2.477
2	66				
1.4	67.2	28.12	2.103	49.42	2.425
'Bat2'					
16	80				
8	104	7.708	2.18	15.23	2.47
4	124	30.687	2.12	40	2.42
2	155				
'Bat3'					
8	46.4	6.57	2.228	9.05	2.534
4	60	11.05	2.164	17.87	2.393
2	72				
'Bat4'					
44	88	1.676	2.55	2	2.75
22	202.4	6.25	2.29	8.68	2.52
4	308	47.148	2.055	95.4	2.47
'Bat5'					
24	156	6	2.3	10.98	2.666
18	184.5	7	2.255	12.65	2.633
10	230.8	18.42	2.155	30	2.589
5	262.1	33.93	2.122	70	2.489

The values of root mean square error (RMSE) [3] that indicate of the models performance to represent the battery behavior during the processes are given in Table 5 calculated with the equation:

$$\mathrm{RMSE} = \left[\frac{1}{N}\sum_{i=1}^{N}\left[\frac{C_i - M_i}{M_i}\right]^2\right]^{1/2} \times 100 \qquad (27)$$

where C_i and M_i are the computed values and measured, respectively and N is the number of point of the measured values.

The Monegon model is not adapted to represent the process of discharge. A higher value of 'RECM' is observed. Concerning the process of charge, the calculated errors show the inefficiency of this model in the description of the process itself, and even in the phenomenon of overcharge. The term included in the Monegon model for the overcharge does not reproduce this process and the error values show this deviation clearly. These great variations are due probably to the value of the various parameters which are identified for another type of battery under different operational conditions, or can be that the batteries used for the description of this model are different from those used in the photovoltaic applications. This model suggested does not refer to a specific type of battery, it refers only that the batteries used are with acid lead. The alloy of the plates

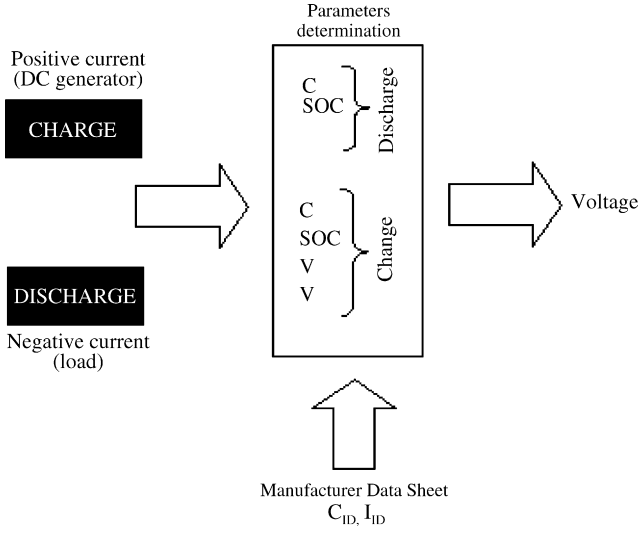

Fig. 9. Synopsis of battery model.

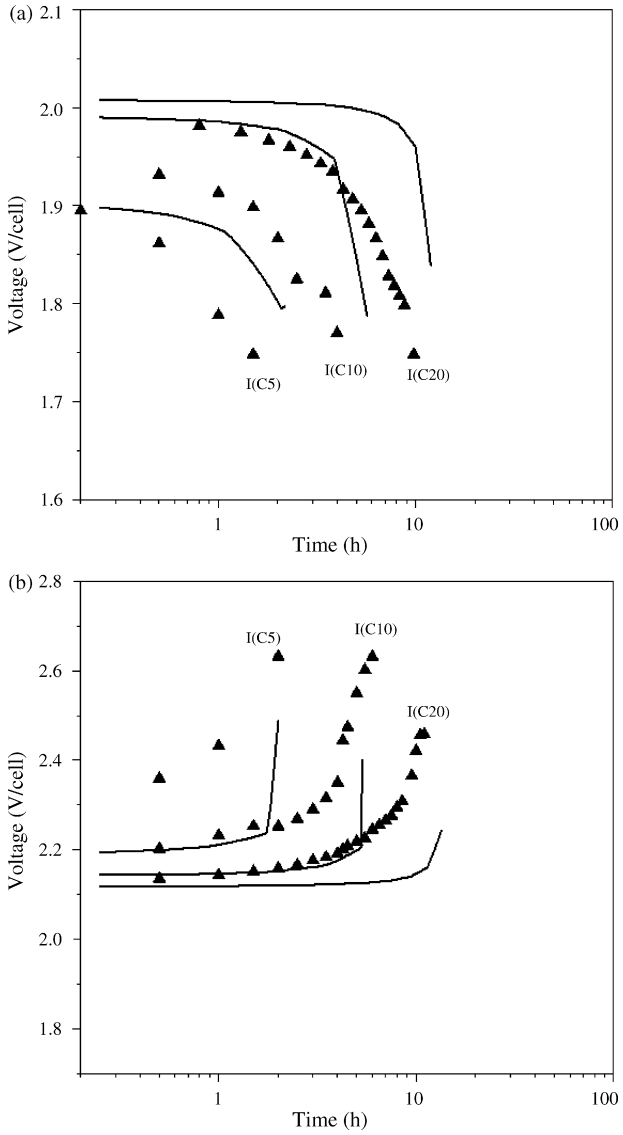

Fig. 10. Monegon model fitting for discharges and charges at various currents and 25 °C for 'Bat1'. (a) Discharge; (b) Charge.

Table 5
Models fitting for charge and discharge processes at $T = 25\,^{\circ}C$

	Models			
	Monegon		CIEMAT	
	Discharge	Charge	Discharge	Charge
RMSE (V/cell)				
'Bat1'	0.052	0.061	0.022	0.021
'Bat2'	0.025	0.059	0.029	0.045
'Bat3'	0.033	0.062	0.010	0.047
'Bat4'	0.044	0.041	0.028	0.024
'Bat5'	0.011	0.043	0.018	0.022

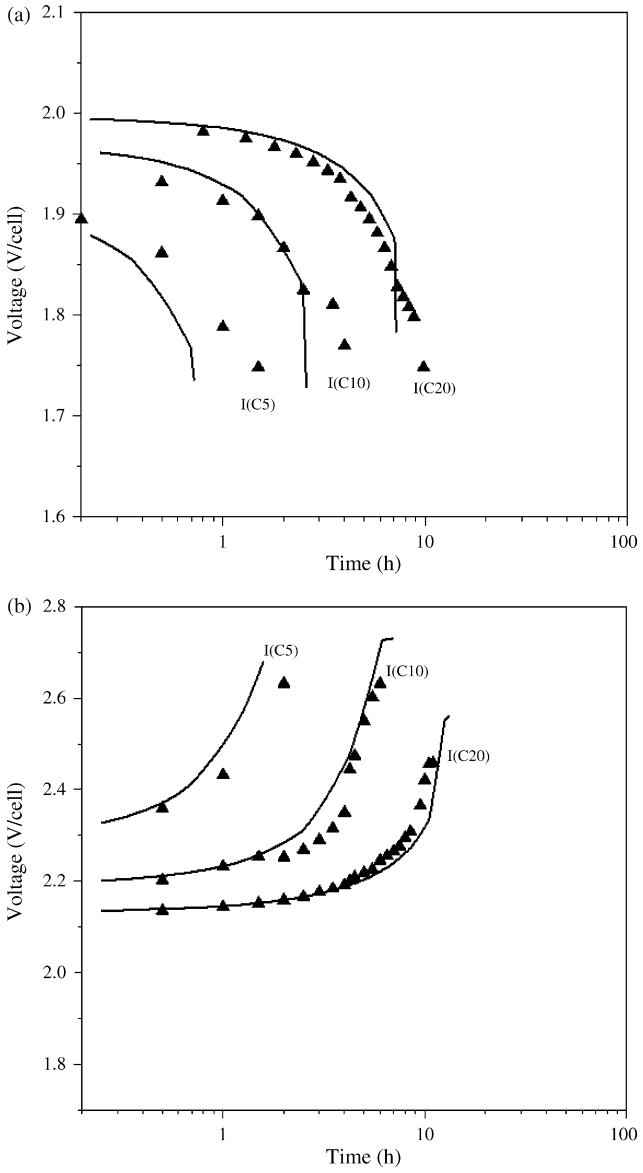

Fig. 11. CIEMAT model fitting for discharges and charges at various currents and 25 °C for 'Bat1'. (a) Discharge; (b) Charge.

is with lead calcium and the mode of discharge is very weak, the rated capacity is C_{500}. However, it is possible to improve this model by substitution of new values of these parameters according to the experimental data, and by inclusion of a term which takes account of the variation of the tension of open circuit with the state of charge of the battery.

The ability of the CIEMAT model to represent the behaviour of the battery is checked by comparing the errors calculated by this model compared to the other model. Also, if we compare the results obtained with those given by Monegon, which follows the same objectives of generalization, we can make the remark that the generalized model of CIEMAT is considerably better. The precision of this standardized model is more than satisfactory, which enables him to approach the majority of the problems currently encountered in the photovoltaic system.

5. Conclusion

This work presents an experimental study for different type of batteries. The two models used for comparison with experimental data are general and can be applied for wide range of lead acid batteries. We analyzed the Monegon model and found that the equation of charge and discharge does not reproduce the experimental curves. Probably the value of parameters was fitted for another type of battery and different operational conditions. The term included in Monegon model for the overcharge does not reproduce these effects and values of RMSE indicate the deviation. The CIEMAT model presents a good performance to represent dynamic and complex battery operation. This is in contrast to Monegon's model; witch presents significant limitations with respect to charging process. In this way, other results could be evaluated considering parameter variations effects in the life of battery. The aging model describing life time of a battery is useful for an economic analysis.

References

[1] C.M. Shepherd, J. Electrochem. Soc. 112 (1965) 657–664.
[2] E.A. Hyman, Report Rd77-1.PSE&G Res. Corp., Newark, NJ, 1977.
[3] W.A. Facinelli, 18th IECEC, 1983, pp. 1582–1588.
[4] D. Mayer, S. Biscaglia, 10th European Photovoltaic Solar Energy Conference, Lisbon, Portugal, 1991, pp. 1209–1213.
[5] H.L. Monegon, Engineering design handbook for stand-alone PV systems, Report no. M108, Monegon Ltd., Gaithersburg, MD, 1981, pp. 28–39.
[6] J.B. Copetti, F. Chenlo, 11th European Photovoltaic Solar Conference, Montreux, Switzerland, 1992.
[7] J.B. Copetti, F. Chenlo, E. Lorenzo, 11th EC Photovoltaic Solar Energy Conference, Montreux, Switzerland, 1992, pp. 1131–1134.
[8] J.B. Copetti, E. Lorenzo an, F. Chenlo, Prog. Photovoltaic Res. Appl. 1 (1993) 283–292.
[9] J.B. Copetti,'Modelado de A cumuladores de Plombo-Acido para Aplicaciones Fotovoltaicas, Tesis Doctoral, Univesidad Politecnica de Madrid, 1993.
[10] H. Bode, Lead Acid Batteries, Wiley and Sons, New York, 1977.
[11] M.A. Laughton, D.J. Warne, Electrical Engineer's Reference Book, sixteenth ed., Newnes, 2003, pp. 960–978.
[12] M.A. Dasoyan, I.A. Aguf, Current Theory of Lead Acid Batteries, published by Technocopylimited, New York, 1979.
[13] W.B. Gu, C.Y. Wang, J. Electrochem. Soc. 144 (2000) 2910–2922.
[14] J.J. Esperilla, J. Félez, G. Romero, A. Carretero, J. Power Sources 165 (2007) 436–445.
[15] N. Achaibou, Storage of Renewable Energies: Application to the Storage of Photovoltaic Solar energy by Electrochemical Accumulators, Magisterial Thesis, Algeria, 2002.
[16] Handbook for Battery Energy Storage Photovoltaic Power Systems, Bechtel National Inc., San Francisco, CA, 1979, 116 pp.